Microchemical Journal 143 (2018) 331–336

Contents lists available at ScienceDirect

Microchemical Journal

journal homepage: www.elsevier.com/locate/microc

Classifying impurity ranges in raw sugarcane using laser-induced breakdown spectroscopy (LIBS) and sum fusion across a tuning parameter window

Wesley Nascimento Guedes[a], Fabíola Manhas Verbi Pereira[a,b,*]

[a] Institute of Energy Research (IPBEN), Institute of Chemistry, São Paulo State University (UNESP), Araraquara, São Paulo 14800-060, Brazil
[b] Department of Chemistry, Idaho State University, Pocatello, ID 83209, United States

ARTICLE INFO

Keywords:
Sugarcane
Impurities
Bioenergy
LIBS
Chemometrics
Classification

ABSTRACT

The presence in raw sugarcane of low levels of solid impurities from soil particles and green and dry/brown sugarcane leaves is relevant to improving sugar mill production performance. Two ranges of impurities for raw sugar manufacturing processes need to be characterized from 0 to 5 wt% (desired material) and 8 to 10 wt% (undesired material); these ranges are denoted as 1 and 2, respectively. Laser-induced breakdown spectroscopy (LIBS) combined with chemometrics is used to detect chemical elements and different impurity ranges in leached raw sugarcane solutions. The potential use of LIBS based on leached solutions immobilized in a polyvinyl alcohol (PVA) polymer requires approximately 2 h sample preparation time. LIBS data are assigned to the above two impurity ranges using fusion of multiple classifiers. Most classifiers require a training set and optimization of a tuning parameter to select the best model; however, the sum fusion across a tuning parameter window used for classifying the samples in this study is a process that does not require either. The classification results are 97% accuracy for both ranges; 94% and 100% specificity for ranges 1 and 2, respectively; and 100% and 94% sensitivity for ranges 1 and 2, respectively. The classification results indicate potential for future applications in sugarcane refineries.

1. Introduction

The scientific literature lacks methods to determine solid impurities in sugarcane before the raw material is introduced into an industrial stream. This information is indispensable for improving milling efficiency and maximizing the use of raw materials saving time, cost and energy. The impurities in raw sugarcane must be monitored since they decrease profit margins for manufacturers and can compromise the yield and quality of extracted sugarcane juice [1].

The literature contains numerous articles describing the impurities that form during sugar or ethanol production. In this paper, these impurities are referred to as “Type A”. Cole et al. [1], for instance, correlated increases in mechanical plant harvest of unburnt sugarcane with high starch concentrations in raw sugar. Starch, fructose and dextran [2] are examples of impurities that form during sugar and ethanol production processes and can hinder both the crystallization [3] and clarification [4] steps. In addition, high concentrations of chemical elements, such as calcium, magnesium, or compounds, like silica and oxalate, can compromise the crystallization process [5,6].

In addition to impurities that form during industrial processes, impurities can be introduced into the processes; these are referred to as “Type B” in this paper. These impurities are from materials such as soil or large amounts of green or dry/brown vegetal parts of the sugarcane plant, as shown in Fig. 1. As noted in the previous sentences, studies on the characterization of Type B impurities are absent, and this paper addresses this issue.

The diagram in Fig. 1 shows an estimation of the quantities of Type B impurities that come from the sugarcane plant (green and dry/brown leaves) and soil. These values were obtained from technical reports [7,8]. To the best of our knowledge, no data have been published on the total impurity content. However, there is a general consensus that the impurity content is approximately 10 to 20%. The amounts of these materials depend on the sugarcane variety and harvesting system. Over the last 5 years, burnt sugarcane has been banned in several countries, including Brazil. As a result, the amount of Type B impurities has alarmingly increased, causing the industrial process to be unpredictable

* Corresponding author at: Institute of Energy Research (IPBEN), Institute of Chemistry, São Paulo State University (UNESP), Araraquara, São Paulo 14800-060, Brazil.
E-mail address: fabiola.verbi@unesp.br (F.M.V. Pereira).

https://doi.org/10.1016/j.microc.2018.08.030
Received 14 July 2018; Received in revised form 15 August 2018; Accepted 17 August 2018
Available online 18 August 2018

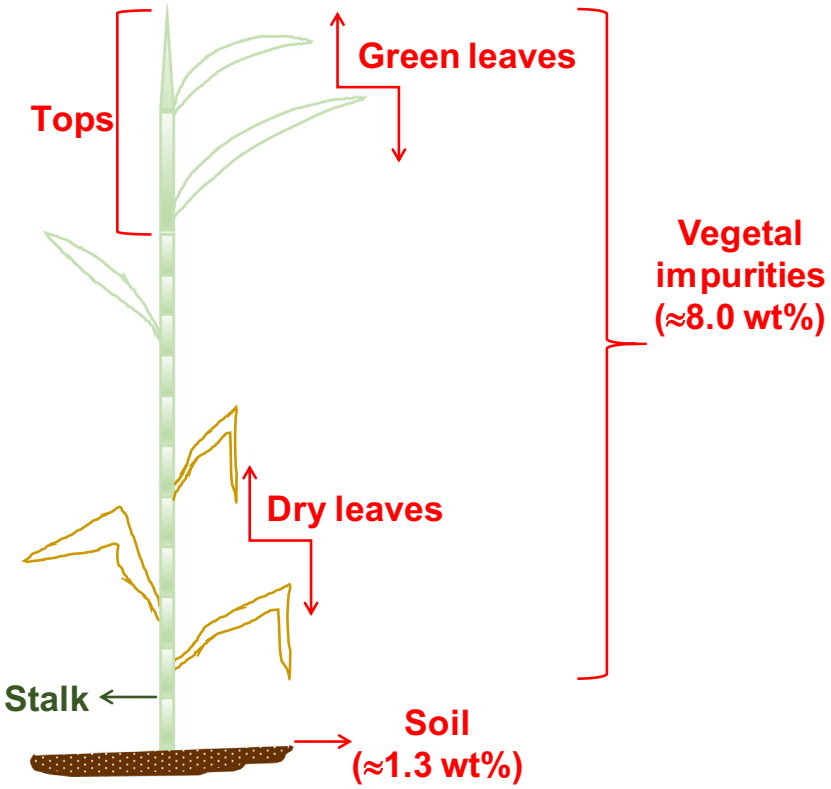

Fig. 1. Diagram of Type B impurities (vegetal parts and soil) and their estimated quantities (wt%) in sugarcane plants denoted by numbers in parentheses.

and difficult to control. Additional drawbacks are the increases in the composition complexity, toxicity and vinasse volume upon the addition of several chemical compounds that are used to establish process control [9]. Currently, no method exists to reduce Type B impurities, and manual stalk separation, which is the most valuable part of the sugarcane plant, is impractical on an industrial process scale.

Sugarcane is a complex plant, and in contrast to potato or beet plants, efficiently cleaning sugarcane on a large industrial scale is not easy. Sugarcane impurities interfere with the milling process and cause damage and energy power losses. Type B impurities can increase the number of dark particles in sugar and the concentrations of starch, dextran and chemical compounds (Type A impurities), ultimately reducing the final product quality.

High-yield sugarcane manufacturing processes depend on raw material characterization [10,11]. The fiber content of sugarcane is routinely determined in industrial facilities and is an important parameter used to calculate grower payments. Juice extraction depends on the fiber content in sugarcane. Thus, establishing an equilibrium between the impurities, mainly Type B, and reliable material introduced in a system is important. Some impurities and fiber are the main constituents of bagasse [12–14], which is used for second-generation energy production [15], plasticizers [16] and biomass [17].

The fiber and impurity amounts introduced in a system (Type B) or formed during an industrial process (Type A) are correlated with the amount and quality of the resultant juice and the yields of the final products, i.e., sugar and ethanol. To rapidly predict the fiber content (%) in raw sugarcane bagasse, laser-induced breakdown spectroscopy (LIBS) has been used in combination with multivariate calibration [12]. The LIBS technique applies a short laser pulse to the sample surface to form a plasma at approximately 10,000 K [18]. The interaction between the plasma and matter produces an emission spectrum, and the spectral information can be used for qualitative and quantitative chemical analyses. In a study published in 2016, Romera et al. [12] used LIBS to determine the fiber content in sugarcane bagasse. The most relevant information from the spectra was selected, and the atomic lines of C, Mg, Na, H, N, K and ionic lines of Ca were used for a partial least squares (PLS) regression analysis. A promising correlation between the reference fiber content values and those predicted by the PLS model was obtained for samples containing moisture [12].

No governmental standard exists for the determination of Type B impurities in raw solid sugarcane materials. The first attempt to establish such a method was published by our research group [19]. This research indicated that the aqueous extracts from sugarcane, soil and green/brown vegetal part mixtures should be studied. The liquid extracts were immobilized using a polyvinyl alcohol (PVA) polymer, and several LIBS emission lines were correlated to the impurity amounts. LIBS is a suitable technique for a direct solid analysis, but Type B impurities are miscellaneous materials with irregular shapes. In this case, the main goal was to immobilize [20,21] aqueous solutions obtained after leaching several solid mixtures. This procedure requires only 2 h of sample preparation time and can be easily incorporated into a sugar or ethanol production chain.

In our previous study, only a qualitative inference about the discrimination of different samples was discussed. The two mixture ranges were divided according to the real conditions of sugarcane crops. For instance, a sugarcane stalk inevitably has some solid dust residues from the field. In Australia, for the clarification and filtration unit operations of raw sugar manufacturing processes, the cane supply soil levels can be between approximately 2 wt% and 10 wt% [22].

An ideal chemometric classification model with a high analytical frequency can be obtained using LIBS emission line spectra as fingerprints [23]. The literature presents several examples of classification techniques, e.g., k nearest neighbor (kNN), soft independent modeling of class analogy (SIMCA), PLS for discriminant analysis (PLS-DA) and linear discriminant analysis (LDA) [24]. Each technique has specific characteristics and can present different prediction classes, including contradictory and inconclusive results. To classify the data, many chemometric methods are available with different criteria to establish

Table 1
Solid fraction compositions for the leached solution dataset.

Mixture	Sugarcane stalk (wt%)	Impurities (wt%)		Sum of Type B impurities (wt%)	Range
		Vegetal parts	Soil		
8	95	5	0	5	1 (n = 25)
9	95	0	5	5	
10	97	3	0	3	
11	97	0	3	3	
12	100	0	0	0	
1	90	10	0	10	2 (n = 35)
2	90	0	10	10	
3	90	5	5	10	
4	92	8	0	8	
5	92	5	3	8	
6	92	3	5	8	
7	92	0	8	8	

the best model. In this study, a sum fusion method across a tuning parameter window, which was introduced by Brownfield et al., was used for data classification by using 17 classification techniques. The outputs of each classifier are normalized across the classes to unit length and summed to obtain a classification consensus, thus providing results with greater confidence [25]. The main advantage is that no thresholds, weights, or training for optimization of classifiers are used to classify the data from a well-established, versatile analytical technique, e.g., the application of LIBS with chemometrics as an analytical method to address an agricultural issue.

2. Materials and methods

2.1. Samples

In this study, a set of 60 leached solution samples was prepared from 12 mixtures composed by sugarcane stalk (desired material) and undesired solid materials (Type B impurities), such as soil and vegetal parts (green and brown). Table 1 presents the compositions of the 12 mixtures; the final content of each sample was 100 wt%. The sampling process consisted of five samples for each mixture described in Table 1. These mixtures were transferred to plastic bags and individually mixed with 200 mL of deionized water at room temperature for 2 h for the leaching procedure. Because the resulting leachates are visually extremely heterogeneous, containing small soil, stalk and leaf particles, from each 200 mL, 50 mL were transferred into plastic flasks. Before each sample collection, the plastic bags were manually mixed for approximately 2 min.

A 200 mg random sample was obtained from each 50 mL sample, and 800 mg 10% (w/v) PVA was added to each sample. This mixture was mixed and transferred to a pre-adapted drying support. After heating for 2 h at 50 °C in an oven, an immobilized sample in solid PVA (leachate) was obtained. The resulting 60 immobilized samples presented thin and plain polymer films suitable for LIBS technique direct analysis [19].

2.2. LIBS dataset

The leachates were measured using a LIBS instrument with a 1064 nm Q-switched Nd:YAG laser (Applied Spectra, Fremont, CA, USA) [19]. The number of independent variables for each spectrum was 12,288 with a resolution between 0.06 and 0.12 nm for the 6-channel charge-coupled device (CCD) spectrometer with a spectral window ranging from 186 to 1042 nm. The laser experimental setup was 80 mJ of laser pulse energy on a 100 μm spot which corresponding to laser fluence of 1000 J/cm^2, at a 5 Hz repetition rate and a 1 mm/s ablation rate. The spectrum acquisition time was 1.05 ms and the delay time was 0.5 μs.

At least 500 LIBS emission spectra were obtained per samples and a data matrix was tested using the mean of these spectra. The spectra were not preprocessed for the calculations. The datasets were evaluated using ranges based on the sum of the fractions of the vegetal parts and soil in wt%; the ranges of 0–5 and 8–10 had 25 and 35 samples, respectively (Table 1). These ranges were divided according to the values expected in sugar factories. A principal component analysis (PCA) of the mean LIBS signals from the leached solutions of raw sugarcane with Type B impurities showed that the samples with between 8 wt% and 10 wt% impurities tended to separate, and the Ca and Mg emission lines had more influence on the segregation than was observed in our prior study [19]. For this study, the impurity ranges between 0 wt% and 5 wt% and between 8 wt% and 10 wt% were defined as ranges 1 and 2, respectively. The first range (from 0 wt% to 5 wt%) represents the material ideally suitable for a production system.

2.3. Data classification

The main goal of sum fusion is to combine the results obtained from 17 classifiers resulting in a classification consensus. The fusion input matrix is the classifiers in the rows and the ranges in the columns. To calculate the sum, raw values in each row are normalized to the unit length for each classifier, in order to eliminate magnitude differences among the output values of the classifiers.

A MATLAB code was applied to calculate the sum fusion classification across the tuning parameter window with 17 classifiers [25]. The tuning parameter window consists of a window of multiple values of number of eigenvectors or nearest neighbors (NNs) or latent variables (LVs) that is used to structure the classifiers in blocks. Table 2 shows six classification methods that require a tuning parameter. In the case of these classifiers the tuning parameter varied from 1 to 23. Eleven classifiers are based on comparing a sample $\mathbf{x}_i$ to the sample class mean $\bar{\mathbf{x}}$, such as cosθ, Euclidean distance, determinant, inner product correlation, unconstrained Procrustes analysis (PA), constrained PA (for 2 classifiers), and extended inverted signal correction difference (EISCD) (for 4 classifiers); no tuning parameter is required and one value is the output matrix for each one.

In this study, the maximum tuning parameter value for the eigenvectors, LVs, and NNs (see Table 2) is 23. For example, for a given classifier, such as the Mahalanobis distance (MD), the MD values are obtained from eigenvector 1, then eigenvectors 1 and 2 for the second window, and 1 to 3 for the third window until the last window, in our case 23. Hence, the maximum window results is 23 in MD classifier. The tuning parameter value is based on the rank of the smallest class where eigenvectors are obtained from the singular value decomposition (SVD) of $\mathbf{X}$.

The classification capability was assessed as the accuracy, specificity, and sensitivity using the following parameters: true positive, false negative, true negative, and false negative. The values of these parameters were calculated using a leave-one-out cross-validation on each

Table 2
Tuning parameter-based classifiers.

Method	Optimized parameter	Tuning parameter window
Partial Least-Squares Discriminant Analysis (PLS2-DA)[a]	Latent variable (LV)	1–23
K Nearest Neighbors (kNN)	Nearest Neighbors (NN)	24–46
Mahalanobis Distance (MD)	Eigenvectors	47–69
sinθ	Eigenvectors	70–92
Q-residual (Q res)	Eigenvectors	93–115
Divergence Criterion (DC)	Eigenvectors	116–138

[a] Pseudo-variables are 1 for in class and –1 for out of class.

Table 3
Description of the selected variables for the dataset composition.

Variables	Emission lines (nm)	Observed elements
1–80	192.87–193.21; 247.58–248.13; 250.72–250.78; 251.45–251.70; 251.95; 252.43–252.50; 252.86–252.92; 279.50–279.73; 279,85–279.90; 280.25–280.42; 285.24–285.29; 288.15–288.26; 385.89–385.97; 387.15; 388.10–388.42; 393.21–393.44; 396.72–396.95; 422.54–422.69; 431.97; 477.09–477.17; 477.55; 479.23; 479.69; 479.91; 480.22–480.44; 480.60–480.67; 480.82–481.13;	C, Ca and Mg
81–320	481.20–487.15; 487.22–490.94; 491.09–491.61; 491.83; 492.05; 492.28; 493.09–493.46; 505.14; 588.71–589.07; 589.12–589.22; 589.33–589.78; 648.23; 648.34; 648.50; 648.71–648.76; 648.87; 648.98; 649.08; 649.24; 649.40; 649.50–651.96;	Na
321–480	652.01–656.06; 656.12–660.06;	H
481–543	660.11–661.68; 661.77–661.82; 661.97; 662.06; 715.56–715.79; 742.11–742.44; 743.85–744.39; 744.61; 746.34–747.42; 747.63; 747.85;	N
544–548	766.39–766.60; 769.81–769.92;	K
549–634	776.19–777.31; 777.42–778.33; 794.64–794.83; 795.03–795.13; 818.34–818.89; 819.54; 820.92–821.66; 822.03–822.40; 824.04–824.32; 844.36–844.71; 862.79–862.95; 867.75–868.62; 870.27–870.35; 871.05–871.21; 871.83; 904.63; 909.50–909.60; 938.62–938.71; 939.16–939.34; 940.59.	O

range shown in Table 1. This process consists of removing one of the samples from a range; then, the calculations are performed on the target sample (removed sample) to be classified using all classifiers. Each sample is removed one by one, and the process is repeated according to the number of samples in each range. The smallest value of the two sums determines to which range a sample belongs [25].

3. Results and discussion

The LIBS system used in this study provides spectra with high dimensionality, i.e., 12,288 variables (186 to 1042 nm) containing thousands of atomic (denoted as I) and ionic (as II) lines, which represent a fingerprint of the chemical composition of leachate samples obtained from the 12 different mixtures ($n = 60$), as described in Table 1. In this study, a variable selection was performed based on the intensities of the emission lines with counts above 40 and high signal-to-noise ratios (SNRs), which included the spectral ranges of Mg II, 279.55 and 280.27 nm; Ca II, 393.37 and 396.85 nm; and K I, 766.49 and 769.90 nm, as shown in Table 3. The referred chemical elements were highly correlated with the samples in PCA for impurities according to our previous study [19]. Other elements were also important for the characterization of samples, such as C I, 193.09 and 247.86; Na I, 589.00 and 589.59; H I, 656.30; N I, 744.23 and 746.83; and O I, 777.42. Consequently, the number of wavelengths was reduced from 12,288 to 634. Fig. 2 shows the fragment profiles of the LIBS spectra after the variable selection. The green and red lines represent ranges 1 (desired material with 0 wt% to 5 wt% Type B impurities) and 2 (undesired material with 8 wt% to 10 wt% Type B impurities), respectively. From the PCA plots shown in Fig. 3a, it is possible to verify a slight tendency of separation for the mean-centered data; however, some samples are overlapped in the first two PCs with 75% of explained variance. Fig. 3b shows the most relevant chemical elements (from 1 to 10) correlated with the ranges of impurities by means of values of loadings using the 634 variables, as described above.

In most cases, to achieve an accurate model, it may be necessary to test more than one algorithm for classifying samples, for example, in the case of overlapping score values for ranges 1 and 2 shown in Fig. 3a. Fig. 4a and b are good examples showing the relevance of combining 17 classifiers. Each interval on the y-axis corresponds to a block of classifiers stacked with its respective output across a window of tuning parameter values (in this study, the window tuning was 23). The target for both examples in Fig. 4 was a sample to be classified as membership of range 1 (0 wt% to 5 wt% impurities). The column sum of the row-wise normalized-to-unit-length values in Fig. 4a (sample of mixture 12 with no impurities added, see Table 1) showed values of 48.3 for range 1 and 137.3 for range 2. In other words, the sum of the row values computed in the majority of classifiers was smaller for range 1 and this sample was correctly classified to range 1. The image in Fig. 4b for a sample of mixture 9, range 1, with 5 wt% soil impurities (see Table 1) shows correct classification to range 1, with the sum of the column values being 90.4 for range 1 and 109.4 for range 2. However, if the classifiers were calculated individually, it would be difficult to obtain the correct range membership for this sample.

Fig. 4c shows that the two classifiers, PLS2-DA and kNN, can achieve good accuracy but depend on the optimized number of LVs or NNs. In PLS2-DA (Fig. 4c), after 3 LVs, a monotonic variation for 95% accuracy is observed, as well as for the other figures of merit. However, there is a discrepancy for kNN (Fig. 4d) after 4 NNs, when the highest value for accuracy is approximately 92%. Nonetheless, in kNN, considering the quality parameters sensitivity and specificity, the number of neighbors is inconsistent. Another implication is that developing a classification model using these methods would require sets for training

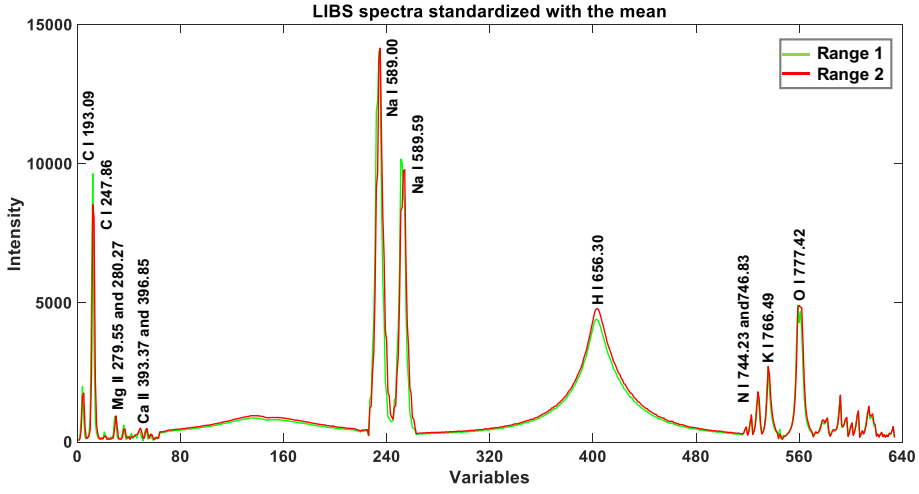

Fig. 2. Average LIBS spectra representing fragment profiles with 634 selected emission lines for samples in ranges 1 (0–5 wt%) and 2 (8–10 wt%) shown by green and red lines, respectively. The most important atomic (I) and ionic (II) emission lines were assigned to chemical elements. (For interpretation of the references to colour in this figure legend, the reader is referred to the web version of this article.)

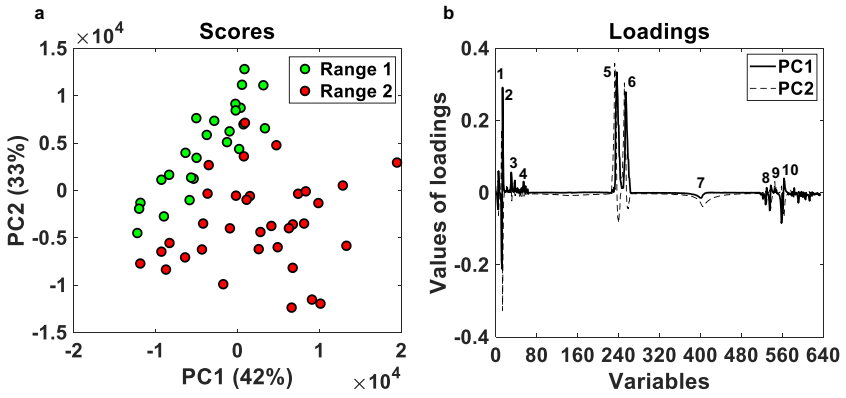

Fig. 3. Scores (**a**) and loadings from a principal component analysis (PCA) performed with 634 selected variables using mean-centered data (**b**). For samples in ranges 1 (0–5 wt%, green circles) and 2 (8–10 wt%, red circles), each number represents the values of loadings for the following emission lines (in nanometers), 1 and 2, C I, 193.09 and 247.86; 3, both Mg II, 279.55 and 280.27; 4, both Ca II, 393.37 and 396.85; 5 and 6, Na I, 589.00 and 589.59, 7, H I, 656.30; 8, both N I, 744.23 and 746.83; 9, K I, 766.49; and 10, O I, 777.42. I and II are atomic and ionic emission lines, respectively. (For interpretation of the references to colour in this figure legend, the reader is referred to the web version of this article.)

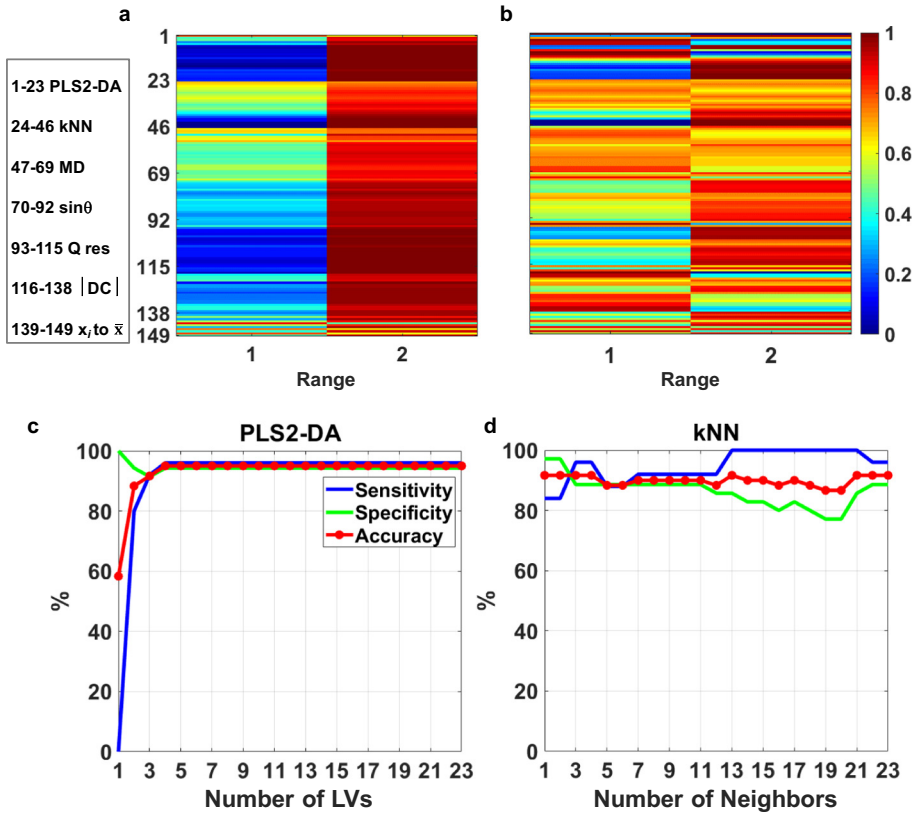

Fig. 4. Representation of classifiers built into the fusion input matrix for classifying a range 1 sample with no impurities added into one of 2 ranges (**a**). The same representation for another sample with 5 wt% soil impurity that actually belong to range 1 (**b**). Each interval represents a window of 23 values for PLS2-DA, kNN, MD, sinθ and Q-res and |DC| and 1 for the classifiers from $\mathbf{x}_i$ to $\bar{\mathbf{x}}$. The raw values in each row are normalized to unit length. Range 1 single classifier results for PLS2-DA and kNN (**c**).

and validation. To overcome this, the fusion process shows no need to select the best tuning parameter window or classifier for the classification for each range. The training could be eliminated since a window of tuning parameter values was used.

The fusion of the classifiers shown in Fig. 5a and b shows slight variations for the classification of quality measures up to the large tuning parameter window of 23. The prior advantage of a fusion method over a single classifier is the ability to make the classification process easy and automatic, with no need for optimization of the tuning window parameter. Additionally, no weights, thresholds or training are required.

High values of the quality parameters were also achieved, independent of the tuning parameter value, as verified in Fig. 5a and b. The accuracy was 97% for both ranges 1 and 2 at the largest possible tuning parameter window. This result suggests the tuning parameter window size can be set to the smallest rank of classes being evaluated and agrees with previous observations [25]. The specificity was higher for range 2 than for range 1; the values were between 100% and 94%, respectively. The sensitivity was 100% for range 1 and 94% for range 2.

4. Conclusions

The new sum fusion classification approach showed that LIBS signals from leached solutions can be used to classify the impurity levels in raw sugarcane without the need to select the best algorithm.

The high values of accuracy, specificity and sensitivity showed the potential for using LIBS emission line fingerprints to identify Type B impurities in raw sugarcane. For both assessed impurity levels, i.e., from 0 to 5 wt% (range 1) and from 8 to 10 wt% (range 2), 97% were accurately classified using sum fusion across tuning parameter windows.

In addition, the combination of LIBS data and this new algorithm is promising for the development of classification models for raw sugarcane impurities from different sources, which would help industrial processes suffer less loss and achieve better control.

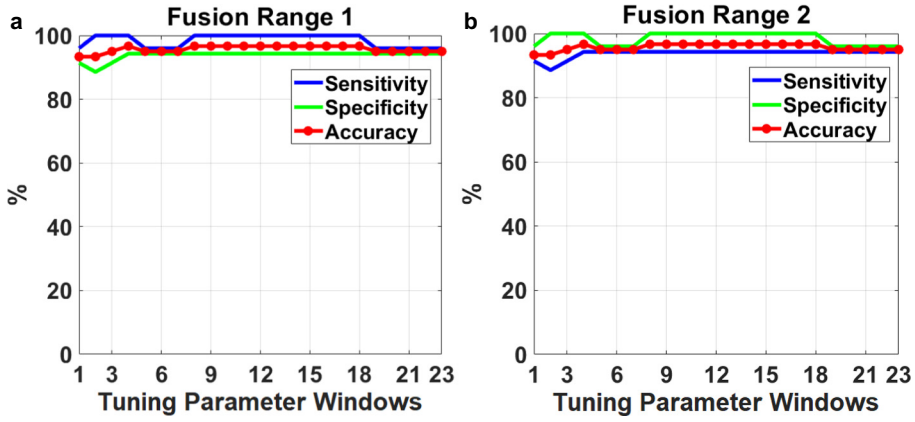

Fig. 5. Classification results and fusion of all 17 classifiers using the mean spectral dataset with 634 variables for range 1 (**a**) and range 2 (**b**). Accuracy (red), specificity (green) and sensitivity (blue). (For interpretation of the references to colour in this figure legend, the reader is referred to the web version of this article.)

Acknowledgments

This study was supported by the São Paulo Research Foundation (FAPESP) under grants Nos. 2016/00779-6 and 2017/05550-0 and, the Coordination for the Improvement of Higher Education Personnel (CAPES) under W.N.G. grant fellowship. The authors are thankfully to Prof. John H. Kalivas for the sum classification code.

References

[1] M. Cole, G. Eggleston, A. Gilbert, I. Rose, B. Andrzejewski, E.St. Cyr, D. Stewart, The presence and implication of soluble, swollen, and insoluble starch at the sugarcane factory and refinery, Int. Sugar J. 115 (2013) 844–851.
[2] P.M. Martins, A. Ferreira, S. Polanco, F. Rocha, A.M. Damas, P. Rein, Unsteady-state transfer of impurities during crystal growth of sucrose in sugarcane solutions, J. Cryst. Growth 311 (2009) 3841–3848.
[3] G.D.A. Merheb, Combined effect of starch and dextran in sucrose crystallization, Sugar Ind. 141 (2016) 697–704.
[4] C.C.D. Thai, W.O.S. Doherty, Characterisation of sugarcane juice particles that influence the clarification process, Int. Sugar J. 114 (2012) 719–724.
[5] W.O.S. Doherty, Effect of calcium and magnesium ions on calcium oxalate formation in sugar solutions, Ind. Eng. Chem. Res. 45 (2006) 642–647.
[6] C.P. East, C.M. Fellows, W.O.S. Doherty, Aspects of the kinetics and solubility of silica and calcium oxalate composites in sugar solutions, J. Food Eng. 117 (2013) 291–298.
[7] Laboratório Nacional de Ciência e Tecnologia do Bioetanol, Estudo revela impurezas minerais da palha de cana-de-açúcar recebida pelas usinas e os efeitos no processamento na indústria, http://ctbe.cnpem.br/publicacoes-ctbe/, (2018) , Accessed date: 25 April 2018.
[8] Nova cana, Os 30 problemas que o mercado sucroenergético precisa enfrentar, https://www.novacana.com/, (2018) , Accessed date: 25 April 2018.
[9] B.S. Moraes, T.L. Junqueira, L.G. Pavanello, O. Cavallet, P.E. Mantelatto, A. Bonomi, M. Zaiat, Anaerobic digestion of vinasse from sugarcane biorefineries in Brazil from energy, environmental, and economic perspectives: profit or expense? Appl. Energy 113 (2014) 825–835.
[10] Y. Everingham, J. Sexton, D. Skocaj, G. Inman-Bamber, Accurate prediction of sugarcane yield using a random forest algorithm, Agron. Sustain. Dev. 36 (27) (2016).
[11] Y. Everingham, J. Sexton, A. Robson, A statistical approach for identifying important climatic influences on sugarcane yields, Int. Sugar J. 118 (2016) 46–50.
[12] J.P.R. Romera, P.L. Barsanelli, F.M.V. Pereira, Expeditious prediction of fiber content in sugar cane: an analytical possibility with LIBS and chemometrics, Fuel 166 (2016) 473–476.
[13] W.S. Carvalho, D.F. Martins, F.R. Gomes, I.R. Leite, L.G. Silva, R. Ruggiero, E.M. Richter, Phosphate adsorption on chemically modified sugarcane bagasse fibres, Biomass Bioenergy 35 (2011) 3913–3919.
[14] N.V. Hoang, A. Furtado, L. Donnan, E.C. Keeffe, F.C. Botha, R.J. Henry, High-throughput profiling of the fiber and sugar composition of sugarcane biomass, Bioenergy Res. 10 (2017) 400–416.
[15] L. Mesa, Y. Martínez, E. Barrio, E. González, Desirability function for optimization of dilute acid pretreatment of sugarcane straw for ethanol production and preliminary economic analysis based in three fermentation configurations, Appl. Energy 198 (2017) 299–311.
[16] H.M. Shaikh, K.V. Pandare, G. Nair, A.J. Varma, Utilization of sugarcane bagasse cellulose for producing cellulose acetates: novel use of residual hemicellulose as plasticizer, Carbohydr. Polym. 76 (2009) 23–29.
[17] G. Eggleston, M. Klich, A. Antoine, S. Beltz, R. Viator, Brown and green sugarcane leaves as potential biomass: how they deteriorate under dry and wet storage conditions, Ind. Crop. Prod. 57 (2014) 69–81.
[18] C. Pasquini, J. Cortez, L.M.C. Silva, F.B. Gonzaga, Laser induced breakdown spectroscopy, J. Braz. Chem. Soc. 18 (2007) 463–512.
[19] D.F. Andrade, W.N. Guedes, F.M.V. Pereira, Detection of chemical elements related to impurities leached from raw sugarcane: use of laser-induced breakdown spectroscopy (LIBS) and chemometrics, Microchem. J. 137 (2018) 443–448.
[20] D.F. Andrade, M.A. Sperança, E.R. Pereira-Filho, Different sample preparation methods for the analysis of suspension fertilizers combining LIBS and liquid-to-solid matrix conversion: determination of essential and toxic elements, Anal. Methods 9 (2017) 5156–5164.
[21] M.A. Sperança, M.S. Pomares-Alfonso, E.R. Pereira-Filho, Analysis of Cuban nickeliferous minerals by laser-induced breakdown spectroscopy (LIBS): nonconventional sample preparation of powder samples, Anal. Methods 10 (2018) 533–540.
[22] G. Sandell, J. Agnew, The Harvesting Best Practice Manual for Chopper Extractor Harvesters, Bureau of Sugar Experiment Stations, Brisbane, Australia, 2002.
[23] F.M.V. Pereira, D.M.B.P. Milori, A.L. Venâncio, M.S.T. Russo, P.K. Martins, J. Freitas-Ástua, Evaluation of the effects of *Candidatus Liberibacter* asiaticus on inoculated citrus plants using laser-induced breakdown spectroscopy (LIBS) and chemometrics tools, Talanta 83 (2010) 351–356.
[24] B.K. Lavine, W.S. Rayens, Classification: basic concepts, in: S.D. Brown, R. Tauler, B. Walczak (Eds.), Comprehensive Chemometrics: Chemical and Biochemical Data Analysis, 3 Elsevier, Amsterdam, The Netherlands, 2009, pp. 507–515.
[25] B. Brownfield, T. Lemos, J.H. Kalivas, Consensus classification using non-optimized classifiers, Anal. Chem. 90 (2018) 4429–4437.